Efficient Hybrid Spatial and Spectral Techniques in Analyzing Planar Periodic Structures with Nonuniform Discretizations

Yongxue Yu and Chi Hou Chan

***Abstract*—A new efficient technique for analyzing planar periodic structures with arbitrary unit cell geometry rendered in a nonuniform discretization is proposed in this paper. The mixed potential integral equation is solved by the method of moments in conjunction with the Rao–Wilton–Glisson triangular discretization. The convergence of computing each element in the impedance matrix is accelerated using Ewald's method for contributions of quasi-dynamic and complex images and the lattice-sum method for the surface-wave contribution. Numerical efficiency and accuracy of this hybrid method are compared with the spectral-domain method.**

***Index Terms*—Convergence of numerical methods, frequency-selective surfaces, periodic structures.**

I. Introduction

ELECTROMAGNETIC analysis of planar periodic structures has a wide range of applications. The spectral-domain method of moments (MoM) is a powerful tool in analyzing periodic structures. However, each element of the impedance matrix still requires the sums of tens of thousands of Floquet's modes. To improve the flexibility in modeling various geometries, a nonuniform discretization was reported in [1], which is an extension of the approach in [2], and the required Green's function is obtained using the complex image method (CIM) [3]. The number of terms for convergence is on the order of several hundreds. In this paper, we show that the numerical efficiency can be further improved by using Ewald's method [4] and the lattice-sum method. Ewald's method has been applied to the free-space Green's function in [5] and the geometry is limited to rectangular elements only. According to the CIM, we decompose the periodic spatial Green's function into three sums, which represent the contributions from the quasi-dynamic images, complex images, and the surface waves, respectively. It is still very time consuming to calculate these sums since most of them are highly oscillating and slowly convergent. The contributions from the quasi-dynamic images, complex images, and surface waves can be accelerated by Ewald's method and the lattice-sum method [6], respectively. These techniques are then integrated to yield an efficient hybrid methodology for analyzing periodic structures.

Manuscript received June 5, 1998. This work was supported by the Hong Kong Research Grant Council under Grant 9 040 270-570.

The authors are with the Wireless Communications Research Center, Department of Electronic Engineering, City University of Hong Kong, Kowloon, Hong Kong (e-mail: eechic@cityu.edu.hk).

Publisher Item Identifier S 0018-9480(00)08716-0.

II. Fast Convergent Series Using Ewald's Method and the Lattice-Sum Method

Employing the CIM, the closed-form spatial Green's functions for the vector and scalar potentials are represented by the summations of three terms, representing the quasi-dynamic images, complex images, and surface wave terms, respectively [7]. Ewald's method involves splitting a sum into two parts using an exponentially converging function: with one over the spatial domain and the other transformed to the spectral domain. The evaluation of the Green's function for the quasi-dynamic images has been presented in [4], [5], where Ewald's method was applied only to the quasi-dynamic images. The essential formula is

$$\frac{e^{-jk_0R_{mn}}}{R_{mn}} = \frac{2}{\sqrt{\pi}}\int_0^\infty \exp\left(-R_{mn}^2 s^2 + \frac{k_0^2}{4s^2}\right) ds. \tag{1}$$

Choosing the integration path suitably, the Green's function can be split into two parts as follows:

$$\begin{aligned} G^{A,q}(x,y,x',y') &= \frac{1}{4\pi}\sum_{m=-\infty}^{\infty}\sum_{n=-\infty}^{\infty} e^{j(k_x^i mT_x + k_y^i nT_y)}\frac{e^{-jkR_{mn0}}}{R_{mn}} \\ &= G_1 + G_2 \end{aligned} \tag{2}$$

$$R_{mn} = \sqrt{(x-x'+mT_x)^2+(y-y'+nT_y)^2+d^2}. \tag{3}$$

Applying Poisson's summation formula and Ewald's identity, following the notations in [4], the spectral and spatial component of the Green's function G_1 and G_2 are given, respectively, as

$$\begin{aligned} G_1(x,y) &= \frac{e^{-j\left[k_x^i(x-x')+k_y^i(y-y')\right]}}{8T_xT_y} \\ &\quad\times \sum_{m=-\infty}^{\infty}\sum_{n=-\infty}^{\infty}\sum_{\pm}\frac{e^{\pm 2d\Omega_{mn}}\operatorname{erfc}(\Omega_{mn}/E_0 \pm dE_0)}{\Omega_{mn}} \\ &\quad\times e^{-j\left[\frac{2m\pi(x-x')}{T_x}+\frac{2n\pi(y-y')}{T_y}\right]} \end{aligned} \tag{4a}$$

$$\begin{aligned} G_2(x,y) &= \frac{1}{8\pi}\sum_{m=-\infty}^{\infty}\sum_{n=-\infty}^{\infty} e^{j(k_x^i mT_x + k_y^i nT_y)} \\ &\quad\times \frac{1}{R_{mn}}\sum_{\pm} e^{\pm jk_0\sqrt{\varepsilon}R_{mn}}\operatorname{erfc}\left(R_{mn}E_0 \pm \frac{j\sqrt{\varepsilon}k_0}{2E_0}\right). \end{aligned} \tag{4b}$$

In this paper, we extend Ewald's method to evaluate complex image terms. The important consideration is that we need to include the contribution from the phase of R_{mn} when choosing the integral path. The path of integration must be chosen so that the integrand remains bounded as $s \to 0$ and decays as $s \to \infty$. Thus, we have

$$s \to \infty, \quad \arg(s) \in \left[-\frac{\pi}{4}-\arg(R_{mn}), \frac{\pi}{4}-\arg(R_{mn})\right] \tag{5}$$

$$s \to 0, \quad \arg(s) \in \left[-\frac{3\pi}{4}+\frac{\beta}{2}, -\frac{\pi}{4}+\frac{\beta}{2}\right], \qquad \beta \equiv \arg(\varepsilon). \tag{6}$$

The correct integration path must be located inside the intersection of (5) and (6). There are six overlapping regions for different β and R_{mn}, as detailed in [7].

The lattice-sum method introduces a lattice sum to represent the Green's function for the surface-wave contribution in terms of a rapidly convergent Neumann series. The surface wave contribution for the two-dimensional periodic Green's function can be represented in terms of zeroth-order Hankel functions of the second kind, as in (7). Meanwhile, it can also be represented by its spectral form, as in (8)

$$G_{sf}^{A,q} = \frac{j\pi}{2} \sum_{m=-\infty}^{\infty} \sum_{n=-\infty}^{\infty} H_0^{(2)}(k_0 \lambda_{mn} \rho_{mn}) e^{j(k_x^i m T_x + k_y^i n T_y)} \tag{7}$$

$$\tilde{G}_{sf}^{A,q} = \frac{2\pi}{T_x T_y} \sum_{m=-\infty}^{\infty} \sum_{n=-\infty}^{\infty} \frac{1}{\gamma_{mn}} e^{j\left[(x-x')\alpha_m + (y-y')\beta_n\right]}. \tag{8}$$

By equating the spatial and spectral expressions in (7) and (8), after some mathematical manipulations, the lattice sum of order l is obtained as [6]

$$S_l(k_0) = \sum_{m=-\infty}^{\infty} \sum_{n=-\infty}^{\infty} H_0^{(2)}(\lambda_{mn} k_0 \rho_{mn}) e^{jl\phi_{mn}} \times e^{j(k_x^i m T_x + k_y^i n T_y)}. \tag{9}$$

We split the lattice sum in (9) into two parts, denoted by Bessel functions of the first kind J and the second kind Y, respectively, as

$$S_l(k_0) = S_l^J(k_0) + jS_l^Y(k_0). \tag{10}$$

Substituting (9), (10) into (7), we have the Green's function as

$$\begin{aligned} G_{sf}^{A,q}(\rho_{mn}) &= \frac{j\pi}{2} H_0^{(1)}(k_0 \rho_{mn}) \\ &\quad + \frac{j\pi}{2} \sum_{l=-\infty}^{\infty} S_l(k_0) J_l(k_0 \lambda_{mn} \rho_{mn}) e^{-jl\phi_{mn}} \\ &= -\frac{\pi}{2} Y_0(k_0 \rho_{mn}) \\ &\quad - \frac{\pi}{2} \sum_{l=-\infty}^{\infty} S_l^Y(k_0) J_l(k_0 \lambda_{mn} \rho_{mn}) e^{-jl\phi_{mn}}. \end{aligned} \tag{11}$$

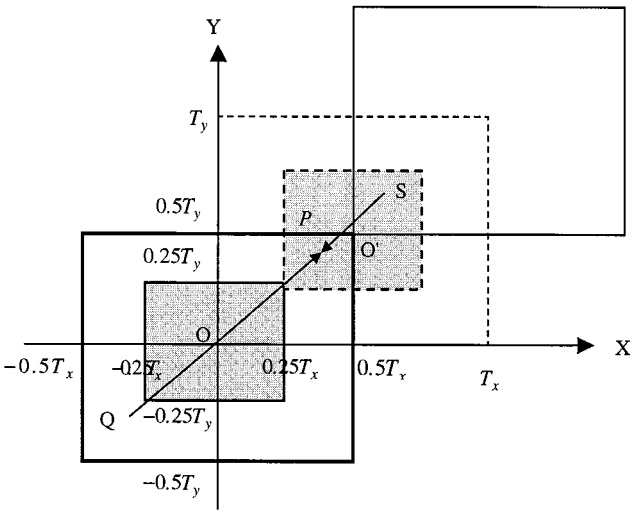

Fig. 1. Modification of the coordinates in the application of the lattice-sum method.

TABLE I
DETAILS OF CONVERGENCE FOR THE PROPOSED METHODS (EXAMPLE 1–3)

Summation Index (K)	Green's Function		Required CPU (Second)
	Amplitude	Phase(Degree)	
Example 1 (Quasi-dynamic images)			
1	0.2995720	-79.23332	8.326e-4
2	0.3152400	-76.26852	3.332e-3
3	0.3151226	-76.28632	7.497e-3
4	0.3151229	-76.28632	1.416e-2
176 (Spectral Method)	**0.3151439**	-76.28700	**8.944**
Example 2 (Complex images)			
1	0.2414714	-167.5280	1.666e-3
2	0.2400956	-170.8593	3.332e-3
3	0.2400663	-170.8581	7.497e-3
4	0.2400663	-170.8581	1.416e-2
4 (Spectral Method)	**0.2400663**	-170.8580	**1.666e-3**
Example 3 (Surface waves)			
1	2.877640	0.8964027	8.334e-4
2	2.876710	0.8966923	8.334e-4
3	2.876719	0.8950125	1.667e-3
4	2.876712	0.8950116	1.667e-3
114 (Spectral Method)	**2.876408**	**0.8945202**	**1.264**

TABLE II
COMPARISON OF NUMBER OF THE TERMS AND REQUIRED CPU (EXAMPLE 1–3)

EXAMPLES	CONVERGENCE TERMS (N)		REQUIRED CPU (SECOND)	
	SPECTRAL METHOD	PROPOSED METHOD	SPECTRAL METHOD	PROPOSED METHOD
Example 1	124609	49	8.944	7.497e-3
Example 2	81	25	1.666e-3	3.332e-3
Example 3	52441	25	1.264	8.329e-4

In this way, the Green's function is represented as a Newmann series with coefficients given by $S_l^Y(k_0)$. Applying the addition

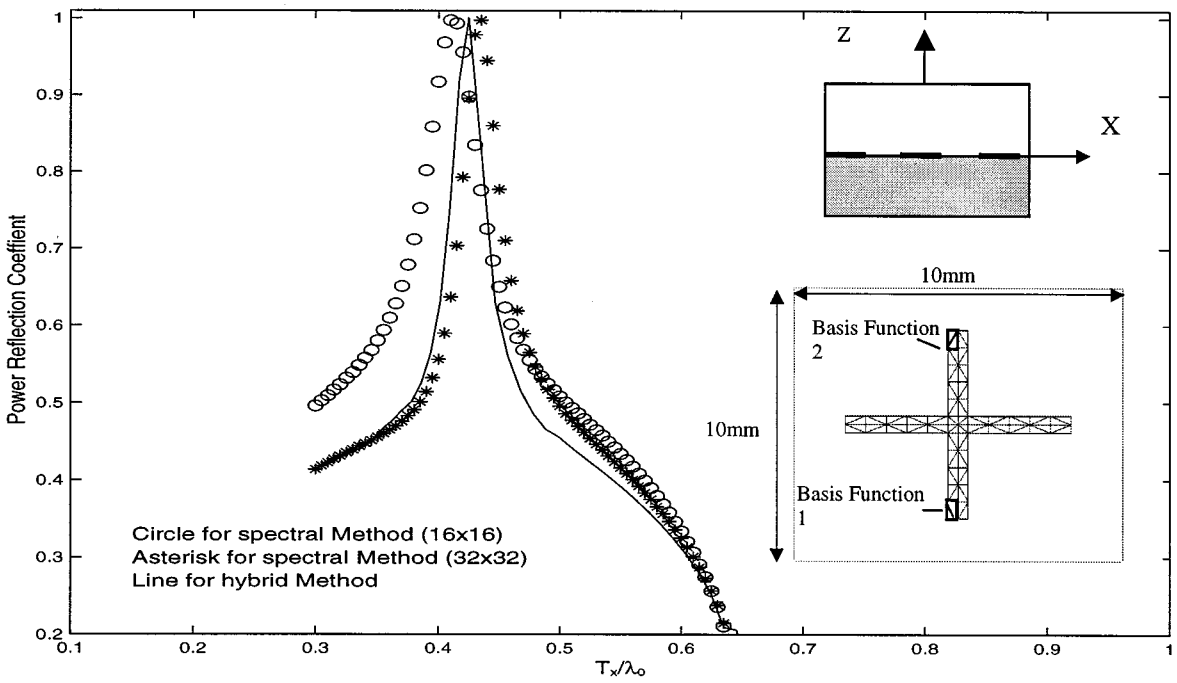

Fig. 2. Comparison of the reflected power from the crossed dipoles of two different methods.

theorem for Bessel and Hankel functions, (9) can be represented by the rapidly converging series [6]

$$S_l^Y(k_0)J_{l+m}(k_0) = -\left[Y_m(k_0)+\frac{1}{\pi}\sum_{k=1}^{m}\frac{(m-k)!}{(k-1)!}\left(\frac{2}{k_0}\right)^{m-2k+2}\right]\delta_{l,0} - 4j^l\sum_p\sum_q\left(\frac{k_0}{\sqrt{\alpha_p^2+\beta_q^2}}\right)^m\frac{J_{l+m}\left(\sqrt{\alpha_p^2+\beta_q^2}\right)}{\alpha_p^2+\beta_q^2-k_0^2}e^{jl\theta_{pq}}. \tag{12}$$

Note that one advantage of this method is that $S_l^Y(k_0)$ is the same for all locations ρ_{mn}. This enables us to construct a table for different orders of l and then to apply this table to all the Green's functions with different ρ_{mn}. It is worth mentioning that in [6], this technique is valid only within a specific range ($0<|x-x'|\le 0.5T_x$ and $0<|y-y'|\le 0.5T_y$). However, it is noted that for those points falling beyond the specific range, the Green's function is evaluated first by using the same method as in [6], and then multiplying a phase-shifting factor. For example, to apply the formula in (12) for an interaction between point Q and P (Fig. 1), we consider this interaction equivalently as that between point S and P. Inside a new cell with central point $O\ (0.5T_x, 0.5T_y)$, this interaction falls into the valid range. A phase shifting factor $e^{j(\alpha_0 T_x+\beta_0 T_y)}$ is then multiplied with the computed result.

To improve the efficiency of constructing the impedance matrix, four interpolation tables are constructed here. The first two tables correspond to the sums in (4), with the phase factor $e^{j(k_x^i mT_x+k_y^i nT_y)}$ excluded for both the quasi-dynamic and complex images, respectively. One of them has the singularity term $1/r$ subtracted. Another two tables correspond to (12) for the surface-wave contribution. Again, one has the singularity $1/\sqrt{k_0\rho_{mn}}$ subtracted, which comes from $Y_0(k_0\rho_{mn})$.

III. Numerical Results

In the first example, the convergence of Ewald's method for a quasi-dynamic image is compared with that of the spectral-domain method. $\theta=45°$, $\phi=25°$, $T_x=1.0\lambda$, $T_y=1.0\lambda$, $x-x'=0.48\lambda$, $y-y'=-0.91\lambda$, $(z-z'+jb)=0.002$, and $\varepsilon_r=1.0$. The index k denotes that the sum runs from $-k$ to k for both m and n. Ewald's method converges at $k=3$ while the spectrum sum oscillates until $k=176$. The accuracy of Ewald's method has reached seven significant figures at $k=3$ and the result agrees with that of the spectral one to the fourth decimal place. The second example computes a practical complex image, which was obtained by Prony's method. The parameters used are $\theta=45°$, $\phi=30°$, $T_x=1.0\lambda$, $T_y=1.0\lambda$, $x-x'=1.9\lambda$, $y-y'=1.9\lambda$, and $(z-z'+jb)=0.14309+j0.45817$. Ewald's method converges at $k=2$, while the spectral method converges at $k=4$. The third example compares the lattice-sum method and the spectral representation of the surface wave term with $\theta=45°$, $\phi=30°$, $T_x=1.0\lambda$, $T_y=1.0\lambda$, $x=0.17\lambda$, $y=0.17\lambda$, $x'=0.14\lambda$, $y'=0.14\lambda$ $K_p=1.23\lambda$, and $\varepsilon_r=1.0$. The index is $p=q=3$ and $m=1$, respectively. The lattice-sum method converges at $k=2$, while the spectral method oscillates until $k=114$ to the fourth decimal place. The details of the convergence comparison for Example 1–3 are listed in Table I. The number of terms for convergence N and the required CPU time to achieve the convergence on a workstation Alpha Server 4100 are given in Table II for each case.

Using this hybrid method, the reflected power for a frequency-selective surface (FSS) with crossed dipoles (Fig. 2) is computed in Example 4, where $\theta=0°$ $\phi=0°$, $T_x=10$, mm,

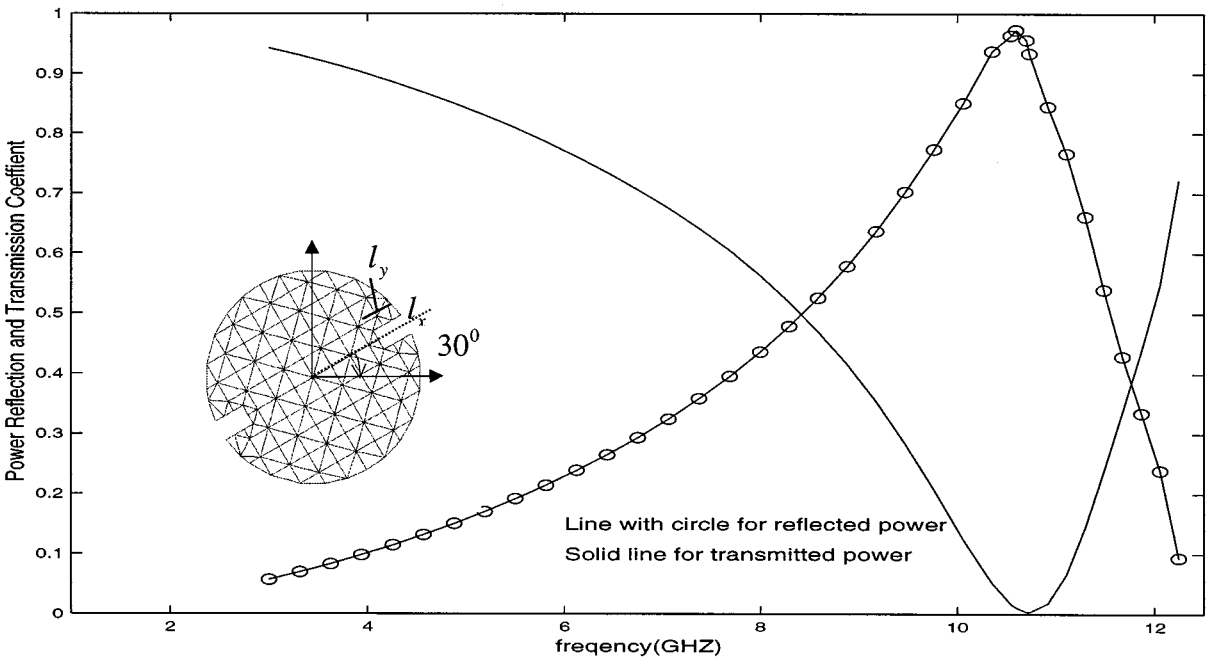

Fig. 3. Discretization of a circular notched patch FSS and the reflected and transmitted power.

TABLE III
COMPARISON OF CONERGENCE AND THE REQUIRED CPU OF TWO METHODS

Method	Summation index	z_{11}	z_{12}	CPU(second)
Spectral	K=200	0.1960+j 255.2241	-2.0770e-2-j4.9954e-2	0.5189
method	K=250	0.1960+j255.4642	-2.0769e-2-j4.9987e-2	0.797
Hybrid	K=2	0.2011+j256.3243	-2.0820e-2-j5.0683e-2	5.39e-2
method	K=3	0.2011+j256.3241	-2.0819e-2-j5.0683e-2	5.65e-2

$T_y = 10$ mm, $\varepsilon_1 = 4.0$ $\varepsilon_2 = 1.01$, $h_1 = 3.0$ mm, $h_2 = 1.0$ mm, and $f = 10$ GHz. The length and width of each arm in the cross is 6.875 and 0.625 mm, respectively. Fig. 2 shows that the numerical result from the hybrid method agrees well with that calculated by the fast Fourier transform (FFT)-based method of discretization of 32×32 in [8], while it has a slight difference from that of 16×16.

In Table III, we compare the spectral and hybrid methods by calculating the impedance matrix elements for two basis functions in the arm of the cross, as shown in Fig. 2. From this table, we see that the hybrid method can accelerate the matrix-filling time to calculate a pair of testing and basis function about 9–15 times. The slight discrepancy between the spectral and hybrid methods is because a true Galerkin procedure is used in the spectral method, while an approximation is applied in the hybrid method [8].

The last example calculates an FSS consisting of notched circular patches. The notch is 60° rotated to the y-axis. The diameter of the patch is 12 mm, and the width and the length of the notch are $l_y = 0.6$ mm and $l_x = 1.8$ mm, respectively. In this example, we have $\theta = 0°$ mm, $\phi = 0°$, $T_x = 20$, $T_y = 20$ mm, $\varepsilon_1 = 2.32$ mm, $\varepsilon_2 = 1.65$, $h_1 = 1.6$, and $h_2 = 1.2$ mm. The Rao–Wilton–Glisson (RWG) discretization is adopted. In Fig. 3, it is shown that the resonance occurs at $f = 10.594$ GHz.

IV. CONCLUSION

In this paper, a new method was proposed to efficiently evaluate the impedance matrix elements in the MoM using the mixed potential integral equation (MPIE) for analyzing periodic structures. This method adopted the CIM to evaluate the closed-form spatial Green's function, and then applied different techniques to accelerate the convergence of the truncated summation. One technique is Ewald's method for evaluating the contributions from quasi-dynamic and complex images, and another is the lattice-sum method, based on an addition theorem of Bessel functions, for that from the surface wave. It is demonstrated by numerical results that the proposed method is much more efficient than the spectral-domain method. In this way, the CIM can be used successfully in periodic structures with complicated geometries.

ACKNOWLEDGMENT

The authors are indebted to Dr. W. Ren, formerly with Kyushu University, Fukuoka, Japan, Dr. R. C. McPhedran, University of Sydney, Sydney, NSW, Australia, and Dr. N. Nicorovici, University of Sydney, Sydney, NSW, Australia, for their helpful discussions.

REFERENCES

[1] R. A. Kipp and C. H. Chan, "A numerically efficient technique for the method of moments solution to planar periodic structures in a layered media," *IEEE Trans. Microwave Theory Tech.*, vol. 42, pp. 635–643, Apr. 1994.

[2] R. E. Jorgenson and R. Mittra, "Efficient calculation of the free-space periodic Green's function," *IEEE Trans. Antennas Propagat.*, vol. 38, pp. 633–642, May 1990.

[3] Y. L. Chow, J. J. Yang, D. G. Fang, and G. E. Howard, "A closed-form spatial Green's function for the thick microstrip substrate," *IEEE Trans., Microwave Theory Tech.*, vol. 39, pp. 588–593, Mar. 1991.
[4] K. E. Jordan, G. R. Richter, and P. Sheng, "An efficient numerical evaluation of the Green's function for the Helmholtz operator on periodic structures," *J. Comput. Phys.*, vol. 63, pp. 222–235, 1986.
[5] A. W. Mathis and A. F. Peterson, "Efficient electromagnetic analysis of a doubly infinite array of rectangular apertures," *IEEE Trans. Microwave Theory Tech.*, vol. 46, pp. 46–54, Jan. 1998.
[6] S. K. Chin, N. A. Nicorovici, and R. C. Mcphedran, "Green's function and lattice sums for electromagnetic scattering by a square array of cylinders," *Phys. Rev. E, Stat. Phys. Plasmas Fluids Relat.*, vol. 49, no. 5, pp. 4590–4602, May 1994.
[7] Y. X. Yu and C. H. Chan, "On the extension of Ewald's method to periodic structures in layered media," *Microwave Opt. Technol. Lett.*, vol. 19, no. 2, pp. 125–131, Oct. 1998.
[8] C. H. Chan and R. A. Kipp, "An improved implementation of triangular-domain basis functions for the analysis of microstrip interconnects," *J. Electromag. Waves Applicat.*, vol. 8, no. 6, pp. 781–797, June 1994.

Yongxue Yu received the B.S. and M.S. degrees in electronic engineering from Sichuan University, Sichuan, China, in 1990 and 1993, respectively, and the Ph.D. degree from the City University of Hong Kong, Hong Kong, in 1999.

From August 1998 to August 1999, she was a Research Assistant in the Wireless Communications Research Center, City University of Hong Kong. Her research interests include electromagnetic characterization of interconnects for electronic packaging, analysis and simulation of interconnects, and periodic structures.

Dr. Yu received was the recipient of the Hong Kong Association of University Women Postgraduate Scholarship (1997–1998).

Chi Hou Chan received the Ph.D. degree in electrical engineering from the University of Illinois at Urbana-Champaign, in 1987.

From 1987 to 1989, he was a Visiting Assistant Professor in the Department of Electrical and Computer Engineering, University of Illinois at Urbana-Champaign. In 1989, he joined the Electrical Engineering Department, University of Washington, Seattle, as an Assistant Professor. In 1993, he became a tenured Associate Professor. In April 1996, he joined the Department of Electronic Engineering, City University of Hong Kong, and was promoted to Professor (Chair) of Electronic Engineering. Since 1998, he has been an Associate Dean (Research) of the Faculty of Science and Engineering, City University of Hong Kong, since 1998. He is also a Guest Professor at Xi'an Jiaotong University. His research focuses on computational electromagnetics. He has authored or co-authored three book chapters, 98 journal papers, and 106 conference papers. He also authored MULTFSS, a general-purpose FSS analysis code currently distributed by DEMACO Inc., Champaign, IL, as part of its McFSS package.

Prof. Chan is a fellow of The Chinese Institute of Engineers (CIE) and the Institution of Electrical Engineers (IEE), U.K. He was a recipient of the 1991 U.S. National Science Foundation Presidential Young Investigator Award.